Optik - International Journal for Light and Electron Optics 201 (2020) 163492

Contents lists available at ScienceDirect

Optik

journal homepage: www.elsevier.com/locate/ijleo

Original research article

Investigation on the scintillation characteristics of CsI(Tl) crystal with Eu dopant: Monte Carlo simulation using GATE code and experimental results

Sajjad Shahmaleki, Faezeh Rahmani*

Department of Physics, K.N. Toosi University of Technology, P.O. Box, 15875-4416, Tehran, Iran

A R T I C L E I N F O

Keywords:
CsI(Tl))
Eu dopant
GATE code
Energy based of light response
Energy resolution

A B S T R A C T

We present new capabilities of the Gate6.2 code that enable the precision simulation of CsI(Tl) and CsI(Tl-Eu) detectors within a comprehensive Monte Carlo code for the first time. Firsty, single crystals were grown by the vertical Bridgman method. A comparison study of the scintillation properties of crystals including energy resolutionand photoluminescence was carried out. Then, the energy response of scintillators was simulated from pulse height spectrum using different gamma sources in the energy range between 32–662 keV. The energy resolutions of CsI (Tl) and CsI(Tl-Eu) at 662 keV were calculated 10.5% and 9.63%, respectively, which were in good agreement with experimental results (10.41% and 9.40%, respectively). The results indicated that GATE code could be an appropriate tool for studying the scintillator's behavior for gamma spectroscopy.

1. Introduction

Today, the use of scintillators has found many significant applications in radiation detection such as industrial controlling, dosimetry, nuclear medicine, medical diagnosis imaging and, so on [1–4]. One of procedures in fabricating a gamma scintillation detector is the crystal growth of scintillator materials with different dopants, which leads different scintillation characteristics. Studying the scintillator behavior with growing different size of crystals as well as with selecting various dopants with different concentrations, and predicting the response function of detector is not always possible only through experimental methods in all situations, so simulation approach based on Monte Carlo techniques can be an appropriate option [5–11]. To perform these studies, a Monte Carlo simulation code should have the ability of producing and transporting the optical photons in a scintillator. Geant4-Gate code is a strong Monte Carlo tool for simulating physical phenomena, which can transport particles in different wavelength ranges, so it can be used for studying the scintillation behavior. The GATE 6.2 software code (Geant4 Application for Emission Tomography) is able to simulate the whole radiation interaction with the scintillator matter including the energy absorption, production, and transport of optical photons [12,13].

CsI(Tl) crystal is one of the most useful scintillator detector due to its density and atomic number as well as the physical characteristics [14]. Light yield, decay time or energy resolution can be improved using added dopants like In, Bi, Yb, Sm, and Eu to its structure [15–19]. In previous works and publications, the scintillation behavior has been investigated only by experimental approaches.

The aim of this paper is to investigate the effect of dopant specially in CsI(Tl) and CsI(Tl-Eu) crystals (studying the Eu as codopant)

* Corresponding author.
E-mail address: FRahmani@kntu.ac.ir (F. Rahmani).

https://doi.org/10.1016/j.ijleo.2019.163492
Received 25 June 2019; Accepted 26 September 2019

on the luminescence and gamma spectra. So, single crystals were grown by the vertical Bridgman method. Also, this work presents the use and validation of GATE for simulating response of CsI(Tl) and CsI(Tl-Eu) detectors. The scintillation behavior of samples in front of different gamma sources has been investigated. The effects of Eu and Tl dopants on the CsI scintillation characteristics have been investigated using GATE 6.2. The simulation results have been compared with related experimental data.

2. Materials and methods

As mentioned, GATE tool has been used for studying the scintillation characteristics of CsI(Tl) as described in next section. For evaluating simulation data, some scintillator crystals have been grown.

The measured gamma spectra have been assessed using photoluminescence and gamma spectroscopy, and scintillation parameters such as energy resolution at different energies of radioactive sources have been measured as described later.

3. GATE simulation

GATE is an advanced open-source code, which employs Geant4 libraries. Geant4 utilizes two models of UNIFIED and GLISUR for the reproducing the scintillation process. In Gate, only UNIFIED model is used in this research, which describes the photon physics upon incidence on surfaces. In a scintillator crystal, optical photons are produced and transported up to the photocathode. It is necessary to determine and to define the scintillation properties including light yield, quenching time, and emission wavelength in the optical simulation. Also, optical features of all materials and surfaces such as refractive index and polished surfaces should be defined. To investigate the reflection type, the Teflon tape as a diffuse reflection candidate was studied. The relative reflectivity of Teflon tape is about 0.98 [20,21]. The refractive index of the materials was considered as wavelength dependent spectra [22,23]. As mentioned before, all simulations have been performed through Gate 6.2 [13]. Here, the important parameter is the light emission spectrum from the scintillator. The emission spectrum of the scintillator sample has been defined as a function of energy in the range of 350–650 nm. So, variations in spectra can be related to the emission spectra of the samples and types of dopants.

The essential properties of the CsI detector have been simulated according to Table 1. The average light yield for this detector has been calculated more than 50,000 optical photons in the given wavelength range for absorption of a 1-MeV photon [14,24,25]. In order to considering the effect of energy resolution due to the statistical fluctuation in simulations (in detector and electronic components, noise, drift and so on) according to the experimental conditions, “RESOLUTIONSCALE” has been considered. This parameter is used in GATE code to confirm the simulated resolution and the real one according to the real characteristics of detector.

Since in the experiments, the scintillator samples have been measured with polished surface, thus the effect of reflective surface type has been considered in simulations.

The scintillator coverage in each arrangement has been represented with Teflon. The distance between the isotropic gamma point source and the crystal has been considered 0.5 cm according to the experimental conditions (Fig. 1).

4. CsI crystal growth with various dopants

Simulation results should be validated via experimental results, thus single CsI crystals with Tl and Eu dopants were grown using the Bridgman method. Equal masses of CsI powder were placed in a quartz vessel with the dopants in Table. 2. Fig. 2 shows the designed furnace for crystal growing using Bridgman method.

Materials (from Merck and Aldrich) were weighted and poured inside the quartz vessel (a cylinder with a conical tip and slope of 45°). Since CsI crystals should be grown in a vacuum (10^{-4} mbar), the mixture was placed into a quartz capsule. The vessel was inserted in the hottest area of the furnace for two hours until all the material melted down. Next, the vessel was shifted to the areas with lower temperatures. To achieve a uniform distribution of the dopants, the thermal operation was completed in the furnace after the full crystal growth during 24 h at 500 °C. Transparent crystals without any fractures were cut and polished in dimension of $5 \times 5 \times 3\,mm^3$. Then the growth crystals were evaluated by the photoluminescence and gamma spectroscopy.

Table 1
Basic properties of CsI(Tl) and CsI(Tl-Eu) detectors [14,24–26].

Quantity	CsI(Tl)	CsI(Tl-Eu)
Mass density (g/cm3)	4.51	4.51
dimension	$5 \times 5 \times 3\,mm^3$	$5 \times 5 \times 3\,mm^3$
Light/MeV (photons)	50,000	50,000
Refractive index	1.79	1.79
Peak emission wavelength (nm)	550	450,580
Light decay (ns)	1000	1000
RESOLUTIONSCALE	1	1
PMT emission wavelength (nm)	420	420
Reflector	Teflon	Teflon

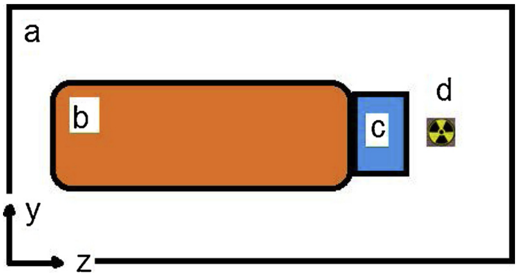

Fig. 1. Detector and PMT configuration in the GATE simulation. (a) air, (b) XP2020 PMT with a diameter of 2 inch, (c) CsI(Tl-Eu) crystal with dimension of $5 \times 5 \times 3\,mm^3$ along z-axis, (d) isotropic point source with distance of 0.5 cm from the detector.

Table 2
Molar mass (%) of dopants in the samples.

Sample	Molar (%) Tl	Molar (%) Eu
CsI(Tl)	0.2	……
CsI(Tl-Eu)	0.2	0.2

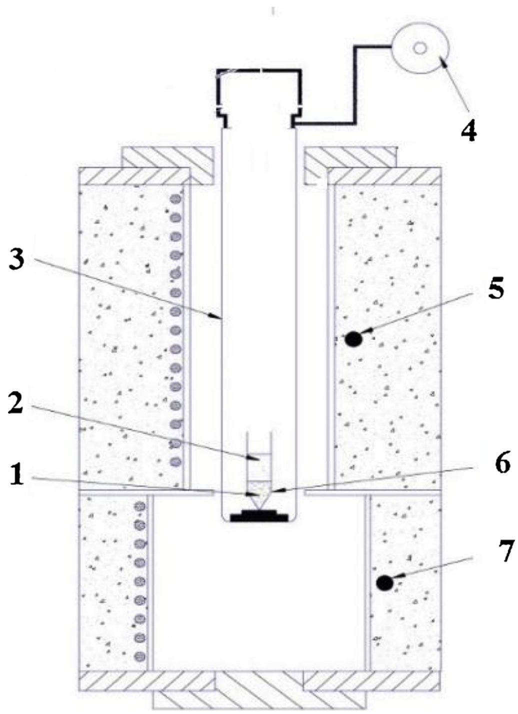

Fig. 2. Schematic view of the furnace used for Bridgman method: 1. Crystal, 2. Melt, 3. Quartz, 4. Pulling 1 mm/h, 5. Hot Zone, 6. Crucible, 7. Cold Zone.

5. Photoluminescence measurement and gamma spectroscopy

The photoluminescence was measured using a LS55-Perkin Elmer system in the wavelength range of 200–800 nm at room temperature. Scintillation properties were assessed with a ^{137}Cs source and the energy resolution of the sample was measured. A photomultiplier tube (PMT) of XP2020 model (Photonics) [25] was used with an opening of 2 inches.

6. Results and discussion

Fig. 3 shows the grown samples excited by a 308-nm wavelength (the maximum excitation wavelength for the crystals). The trends of crystal emission spectra in the range of 350–650 nm are similar and only the intensities (the areas under their peaks) are different. The intensity of the emission spectrum of CsI(Tl-Eu) is lower than that of the CsI(Tl), which is due to the Eu dopant's ions.

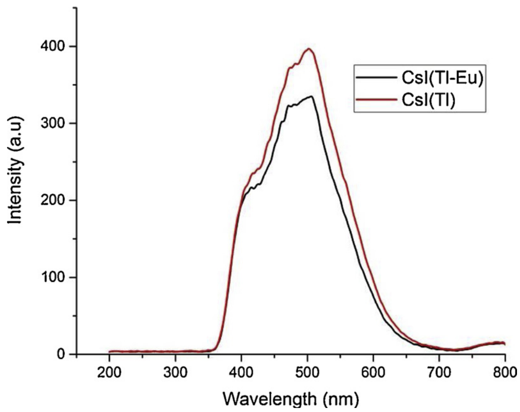

Fig. 3. The emission spectra of crystal samples with single 308-nm wavelength excitation.

Because of forming the Eu sublevel, the emission peak related to the Tl sublevel in the range of 450–500 nm is lower. The light peak of Tl is found at 510 nm, which is in agreement with the results reported in the literatures [26,27].

The Tl content in the CsI(Tl-Eu) sample was equal to the weight ratio of the CsI(Tl), therefore, the CsI(Tl-Eu) emission spectrum shifts to the longer wavelengths relative to the CsI(Tl) sample. The emission spectra at Eu sublevels overlaps with Tl sublevels, thus the increased probability in energy transition in the crystal lattice causes the increased number of photons, and consequently enhanced energy resolution relative to the CsI(Tl) crystal.

Fig. 4 shows the CsI(Tl) and CsI(Tl-Eu) single crystal pulse height spectra from 400 to 900 keV. By coupling them with a Photonics XP2020 PMT, the energy resolution of the 662 keV for the single crystal can be obtained. Based on the experimental results, the energy resolution of CsI(Tl) is 10.41% at 662 keV, which is not as good as that of the standard CsI(Tl), but according to the Tl concentration, it is consistent with a value of 10.6% reported in Ref [26]. As we know, the energy resolution is affected by several factors, such as crystal inhomogeneity, non-proportionality, and the photons, transfer conditions of in the crystal up to the PMT [1–4,27]. The energy resolution of CsI(Tl-Eu) is 9.4% at 662 keV, which is as good as that of the CsI(Tl) in the work, while it is consistent with a value of 9.5% reported in Ref [26]. In the following sections, pulse height spectrum for CsI(Tl-Eu) and CsI(Tl) will be investigated accordingly by GATE code.

Using GATE code, an isotropic ^{137}Cs (energy of 662 keV) gamma point source was placed in front of crystal samples. Fig. 5 and Table 3 show a comparison of the simulated pulse height spectra between CsI(Tl) and CsI(Tl-Eu).

The energy resolution of CsI(Tl) and CsI(Tl-Eu) samples are in good agreement with the experimental results obtained for the 662 keV full energy peak. The energy resolution was simulated from pulse height spectrum measurement using different radioactive sources in the energy range between 32 keV and 662 keV, as listed in Table 4.

The energy spectra of CsI(Tl) and CsI(Tl-Eu) detectors for the chosen isotopes were generated assuming the energy resolution model discussed by Eq. (1). The total energy deposited in the scintillator was also simulated. The best combination for good energy resolution was found for the CsI(Tl-Eu) detector. Fig. 6, Table 5 shows the energy resolution for different gamma ray energies for CsI (Tl) and CsI(Tl-Eu) detectors.

We have used an energy resolution function based on Eq. (1):

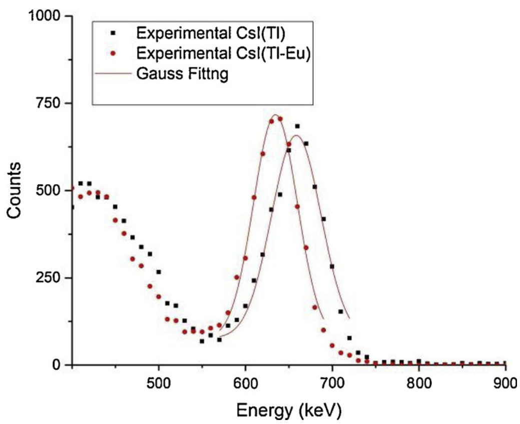

Fig. 4. The pulse height spectra of the samples using ^{137}Cs at 662 keV for counting time of 150 s: The energy resolution of 10.41% for CsI(Tl) and 9.4% for CsI(Tl-Eu).

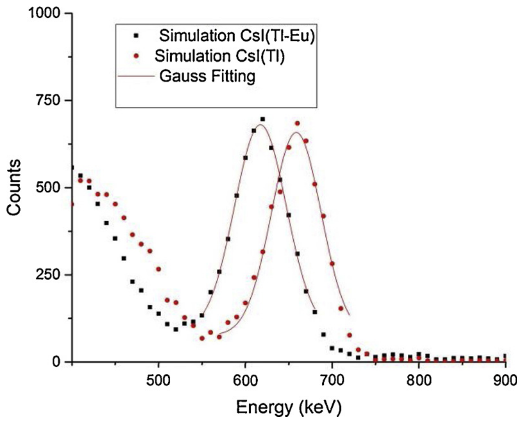

Fig. 5. Simulated pulse height spectrum at 662 keV for counting time of 150 s: Energy resolution of 10.5% for CsI(Tl), and 9.63% for CsI(Tl-Eu).

Table 3
Comparison of the simulated (Sim.) and experimental (Exp.) energy resolution.

Sample	Energy resolution in 662 keV (Exp.)	Energy resolution in 662 keV (Sim.)	Relative error according to experiment (%)
CsI(Tl)	10.41	10.5	0.8
CsI(Tl-Eu)	9.40	9.63	2.44

Table 4
The radioactive sources and gamma energies for simulation.

Source	Energy of gamma ray (keV)	Half-life	Intensity (%)
^{137}Cs	32.1 (K X-ray)	30.04 yrs	3.6
^{241}Am	59.5	432.2 yrs	35.90
^{133}Ba	81	10.52 yrs	34.0
^{109}Cd	88	462.0 day	3.61
^{152}Eu	121	13.5 yrs	28.58
^{152}Eu	244	13.5 yrs	7
^{51}Cr	320.1	27.7 day	9.92
^{22}Na	511	2.60 yrs	179.79
^{207}Bi	568	31.55 yrs	97.7
^{137}Cs	661.6	30.04 yrs	85.10

$$R=\sqrt{\left(\frac{A\sqrt{E}}{E}\right)^2+B^2} \quad (1)$$

where, A and B are the fitting parameters of the simulating relative resolution of R as a function of energy, E. This model can be easily implemented into the experimental and simulation results [14,19].

The simulated energy resolution of the CsI(Tl) and CsI(Tl-Eu) samples, based on the parameters in Table 5, are in good agreement with the experimental results obtained for ^{137}Cs, ^{22}Na, ^{241}Am sources in Table 4. It should be noted that differences in simulation results and experimental tests were less than 6%.

7. Conclusion

In this research, GATE code has been evaluated to use in simulation of scintillation properties. For better conclusion, CsI crystals were grown with Eu and Tl dopants through Bridgman method and scintillation properties were evaluated in order to achieve a desirable function for the gamma detection. The Eu dopant led to enhanced scintillation characteristics in the CsI(Tl) crystal. According to the research (measurements and simulations), the dopant types and concentrations significantly affect the emission spectra and scintillation characteristics. Finally, the energy resolution function has been determined using simulation that leads to the fitting parameters, presenting in the accompanying experimental results in this work. According to the obtained results, Gate code now provides a more flexible environment for the simulation of CsI(Tl) and CsI(Tl-Eu) detectors. This capability should significantly aid users who require a more powerful capability to simulate inorganic scintillation detectors within larger experiments or to computationally evaluate advanced detector designs.

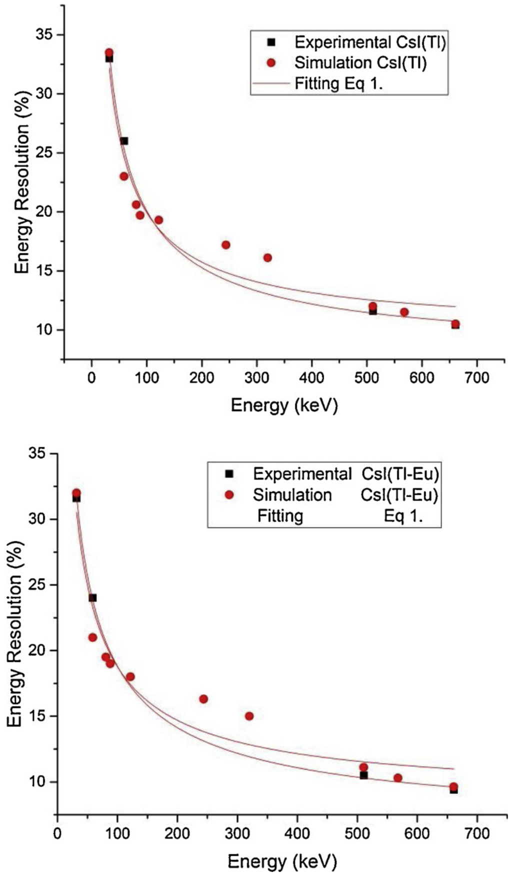

Fig. 6. Energy resolution of CsI(Tl) and CsI(Tl-Eu) single crystal as a function of gamma ray energy.

Table 5
A and B parameters comparison of the simulation (Sim.) and experimental (Exp.) results.

Coefficient	Exp. CsI(Tl)	Sim. CsI(Tl)	Exp. CsI(Tl-Eu)	Sim. CsI(Tl-Eu)
A	184.10	173.10	175.37	165.14
B	7.99	9.89	6.77	8.92

References

[1] T. Jing, C.A. Goodman, J. Drewery, D. Wildermuth, Amorphous silicon pixel layers with cesium iodide converters for medical radiography, IEEE Trans. Nucl. Sci 41 (1994) 903–909.
[2] N. Martin, Scintillation detectors for X-rays", Meas. Sci. Technol. 17 (4) (2006) R37–R54.
[3] J.C. Brice, Crystal Growth Process, (1986).
[4] C.W.E. van Eijk, Inorganic scintillators in medical imaging detector, Nucl. Instrum. Methods Phys. Res. A 509 (2003) 17–25.
[5] Z.S. Hartwig, P. Gumplinger, Simulating response functions and pulse shape discrimination for organic scintillation detectors with Geant4, Nucl. Instrum. Methods Phys. Res. A 737 (2014) 155–162.
[6] S. Crespin, D. De Freitas, P. Brette, A. Falvard, J. Maublant, Assessment of a simulation software for scintillation detector", Nucl. Instrum. Methods Phys. Res. A 527 (2004) 206–210.
[7] K. Hyunki, J. Hyung, B. Kyung, H. Jeon, J. Yulkim, C. Kyukim, G. CHO, The effect of surface roughness of CsI(Tl) micro-columns on the resolution of the X-ray image; optical simulation study, J. Radiat. Prot. Res. 34 (1) (2009) 25–29.
[8] D. Lazaro, I. Buvat, G. Loudos, D. Strul, G. Santin, N. Giokaris, D. Donnarieix, L. Maigne, V. Spanoudaki, S. Styliaris, S. Staelens, V. Breton, Validation of the GATE Monte Carlo simulation platform for modelling a CsI(Tl) scintillation camera dedicated to small-animal imaging, Phys. Med. Biol. 49 (2004) 271–285.
[9] H. Tekin, MCNP-X Monte Carlo code application for mass attenuation coefficients of concrete at different energies by modeling 3 × 3 Inch NaI(Tl) detector and comparison with XCOM and Monte Carlo data, Sci. Technol. Nucl. Install. (2016) 7.
[10] M.T. Hajheidari, M.J. Safari, H. Afarideh, H. Rouhi, Experimental validation of response function of a NaI (Tl) detector modeled with Monte Carlo codes, J. Instrum. JINST 11 (2016) P06011.
[11] N. Jenny, M. Isaksson, A Monte Carlo calibration of a whole body counter using the ICRP computational phantoms, Radiat. Prot. Dosimetry 163 (4) (2015) 458–467.
[12] N. Jenny, V. Cuplov, M. Isaksson, Identifying key surface parameters for optical photon transport in GEANT4/GATE simulations, Appl. Radiat. Isot. 103 (2015) 15–24.
[13] Wiki.opengatecollaboration.org/index.php/Users_Guide_V6.2.

[14] G.F. Knoll, Radiation Detection and Measurement, third edition, Wiley Inc., New York, 2000.

[15] W. Yuntao, R. Guohao, F. Meng, C. Xiaofeng, D. Dongzhou, L. Huanyin, P. Shangke, Ultralow-concentration Sm codoping in CsI:Tl scintillator: a case of little things can make a big difference", Opt. Mater. 38 (2014) 297–300.

[16] L.A. Kappers, R.H. Bartram, D.S. Hamilton, A. Lempicki, C. Brecher, V. Gaysinskiy, E.E. Ovechkin, S. Thacker, V.V. Nagarkar, A tunneling model for afterglow suppression in CsI:Tl,Sm scintillation materials, Radiat. Meas. 45 (2010) 426–428.

[17] D. Totsuka, T. Yanagida, Y. Fujimoto, Y. Yokota, F. Moretti, A. Vedda, A. Yoshikawa, Afterglow suppression by codoping with Bi in CsI:Tl crystal scintillator", Appl. Phys. Express 5 (2012) 052601.

[18] W. Yuntao, R. Guohao, N. Martin, C. Xiaofeng, D. Dongzhou, L. Huanyin, P. Shangke, F. Yang, CsI:Tl^{+},Yb^{2+}: ultra-high light yield scintillator with reduced afterglow, 3312, CrystEngComm 16 (2014) 3312–3317.

[19] W. Yuntao, R. Guohao, F. Meng, C. Xiaofeng, D. Dongzhou, L. Huanyin, P. Shangke, L. Charles, Scintillation characteristics of indium doped cesium iodide single crystal, IEEE Trans. Nucl. Sci. 62 (April 2) (2015).

[20] P. Ghorbani, D. Sardari, R. Azimirad, M. Hosntala, Assessment of optical photon collection in a large plastic scintillator using Geant4-Gate code, Optik 158 (2018) 305–311.

[21] M. Janecek, Reflectivity spectra for commonly used reflectors, IEEE Trans. Nucl. Sci. 59 (3) (2012) 490–497.

[22] E.D. Palik, Handbook of Optical Constants of Solids, Academic Press, USA, 1998.

[23] M.J. Weber, Handbook of Optical Materials, CRC Press, USA, 2003.

[24] www.crystals.saint-gobain.com.

[25] www.photonis.com.

[26] C. Brechera, A. Lempicki, S.R. Miller, J. Glodo, E.E. Ovechkina, V. Gaysinskiy, V.V. Nagarkar, R.H. Bartram, Suppression of afterglow in CsI:Tl by codoping with Eu^{2+}: experimental", Nucl. Instrum. Methods Phys. Res. A 558 (2006) 450–457.

[27] P. Dorenbos, J. de has, C.W.E. van Eijk, Non-proportionality in the scintillation response and the energy resolution obtainable with scintillation crystals, IEEE Trans. Nucl. Sci. 42 (December 6) (1995) 2190–2202.